

Performance of contrast-enhanced ultrasound liver imaging reporting and data system for differentiation of patients at risk of hepatocellular carcinoma and liver metastasis

Wei Qin Huang[#], Ruoxuan Lin[#], Zhongshi Du, Zhougui Wu, Xiaohui Ke and Lina Tang

Department of Ultrasonography, Clinical Oncology School of Fujian Medical University, Fujian Cancer Hospital, Fujian Branch of Fudan University Shanghai Cancer Center, Fuzhou, Fujian, China

ABSTRACT

Background: Hepatocellular carcinoma (HCC) and metastatic liver tumors (MLT) are the most common malignant liver lesions, each requiring distinct therapeutic approaches. Accurate differentiation between these malignancies is critical for appropriate treatment planning and prognostication. However, there is limited data on the performance of contrast-enhanced ultrasound liver imaging reporting and data system (CEUS-LI-RADS) in this differentiation.

Objective: To evaluate the diagnostic efficacy of the CEUS-LI-RADS in distinguishing between HCC and MLT in an expanded population at risk for both tumors.

Methods: Between June 2017 and January 2022, 108 patients with HCC and 138 patients with MLT who were pathologically diagnosed, were included in this retrospective study. Two radiologists independently reviewed the CEUS features and liver imaging reporting and data system (LI-RADS) categories of the lesions, and based on their consensus, we calculated the diagnostic performance, including the area under the receiver operating characteristic curve, sensitivity, specificity, and accuracy of the CEUS-LI-RADS criteria.

Results: The sensitivity, specificity, and accuracy of CEUS LI-RADS category 5 (CEUS-LR-5) for predicting HCC were 49.1% [95% confidence interval (CI) 39.3–58.9], 97.1% (95% CI 92.7–99.2), and 76%, respectively, whereas the corresponding values for LI-RADS category M (LR-M) for diagnosing MLT were 89.1% (95%CI 82.7–93.8), 72.2% (95%CI 62.8–80.4), and 81.7%, respectively. Based on current LR-M criteria, a small proportion of HCCs were classified as LR-M due to the presence of early cessation (45–60s). In the analysis of the MLT subgroup, we found that the tumor size affects the distribution of LI-RADS (LR) classification in the subgroup ($p=0.037$), and LI-RADS category 3 (LR-3) classification was observed more frequently in tumors of small size (≤ 3 cm) than those of larger size. In addition, LR-3 metastases were more frequently characterized by hypovascular supply.

Conclusions: CEUS-LI-RADS demonstrates high specificity in distinguishing HCC from MLT, providing a reliable noninvasive diagnostic tool that can enhance clinical decision-making. These findings are clinically significant as they can improve patient management and treatment outcomes, and they underscore the need for future research to refine and expand the use of CEUS-LI-RADS in diverse clinical settings.

Abbreviations: LI-RADS: Liver Imaging Reporting and Data System; CEUS-LI-RADS: Contrast-Enhanced Ultrasound Liver Imaging Reporting and Data System; HCC: hepatocellular carcinoma; MLT: metastatic liver tumor; CEUS-LR-5: CEUS LI-RADS category 5; CI: confidence interval; LR-M: LI-RADS category M; LR-3: LI-RADS category 3; AUC: area under the receiver operating characteristic curve; CEUS: Contrast-Enhanced Ultrasound; MI: Mechanical Index; AP: arterial phase; APHE: arterial phase hyperenhancement; PPV: positive predictive value; NPV: negative predictive value; BUS: B mode Ultrasound; IHC: immunohistochemistry; TIV: tumor in vein

ARTICLE HISTORY

Received 9 January 2024



Revised 26 May 2024

Accepted 8 November 2024


2024

KEYWORDS

Contrast media; liver neoplasms; ultrasonography

CONTACT Lina Tang  tanglinalina@outlook.com  Department of Ultrasonography, Clinical Oncology School of Fujian Medical University, Fujian Cancer Hospital, Fujian Branch of Fudan University Shanghai Cancer Center, No. 420, Fuma Road, Jin'an District, Fuzhou 350014, China

[#]These authors contributed equally to this study.

 Supplemental data for this article can be accessed online at <https://doi.org/10.1080/07853890.2024.2442072>.

© 2024 The Author(s). Published by Informa UK Limited, trading as Taylor & Francis Group

This is an Open Access article distributed under the terms of the Creative Commons Attribution-NonCommercial License (<http://creativecommons.org/licenses/by-nc/4.0/>), which permits unrestricted non-commercial use, distribution, and reproduction in any medium, provided the original work is properly cited. The terms on which this article has been published allow the posting of the Accepted Manuscript in a repository by the author(s) or with their consent.

Introduction

Metastatic liver tumors (MLT) are frequently found to colonize the liver from tumors of other organs due to their anatomical factors and unique environment [1]. In addition, hepatocellular carcinoma (HCC) comprises more than 90% of cases of non-metastatic liver tumors [2]. Therefore, it is essential to accurately identify these two hepatic malignancies. Patients with chronic hepatitis or liver cirrhosis of various etiologies commonly develop HCC [3]. The contrast-enhanced ultrasound liver imaging reporting and data system (CEUS-LI-RADS) [4] is a valuable tool for noninvasively diagnosing HCC in high-risk patients with a high pretest probability of HCC [5,6].

Both malignant MLT and HCC are primary liver cancers that can show arterial phase enhancement and washout on contrast-enhanced ultrasound (CEUS). However, MLT usually has heterogeneous and irregular enhancement, while HCC usually has homogeneous and well-defined enhancement. MLT also washes out earlier than HCC, the time of enhancement in HCC is longer than that of metastatic cancer, usually up to 20s, while MLT is usually within 10s. MLT can have different CEUS features depending on the type of tumor, such as cholangiocarcinoma, sarcoma, lymphoma, or metastasis. These features may include hypoenhancement, iso-enhancement, rim enhancement, pseudocapsule, target sign, or spoke-wheel pattern. The CEUS features of MLT may also vary according to the degree of differentiation, the presence of necrosis, or the coexistence of HCC [7–9].

However, specific supporting evidence for the application of CEUS-LI-RADS v2017 to differentiate HCC from MLT in patients at risk for both types of tumors has not been confirmed. Arterial hyperenhancement followed by late discharge is the typical feature of the diagnosis of HCC [10]. Despite this, a substantial number of HCCs and MLTs have overlapping features and are classified as LI-RADS category M (LR-M) lesions, which are malignant but not HCC-specific. In addition, a current or past history of extrahepatic primary malignancy may increase the probability of misdiagnosis of HCC as MLT in comparison to patients without such a history.

Consequently, the objective of this study was to evaluate the performance of CEUS-LI-RADS in accurately diagnosing MLT and HCC in a limited study population.

Patients and methods

Patient selection

Our Institutional Review Board approved this retrospective study, and written informed consent was

waived due to its retrospective nature. In this retrospective study, 417 consecutive patients with complete CEUS records between June 2017 and January 2022, were enrolled.

The inclusion criteria were as follows: (1) Liver Lesion Diagnosis: Only patients with liver lesions confirmed as HCC or MLT through surgical resection or biopsy were included. (2) CEUS-LI-RADS Applicability: Participants included those with liver cirrhosis (such as leading by cirrhotic with congenital hepatic fibrosis, vascular disorder, and other diseases), chronic hepatitis B, or a history of HCC, fitting the criteria for CEUS-LI-RADS. (3) Risk of MLT: Patients with a history of any extrahepatic malignancy were included, reflecting the risk for MLT.

The exclusion criteria were: (1) Systemic or local treatment, such as radiofrequency ablation or chemotherapy, administered prior to CEUS; (2) Technical difficulties (e.g. shaky recording, weak ability to hold breath, and ultrasound absorption due to the deep location of the tumor, specifically when the distance between the skin and the tumor exceeds 15cm). When there were multiple liver lesions, only the predominant tumor was selected for cluster sampling bias reduction.

According to our inclusion criteria, we preliminarily included 252 patients. Then, based on our exclusion criteria, we excluded 6 patients, resulting in a final count of 246 patients, among which there were 108 cases of HCC and 138 cases of MLT, as depicted in Figure 1.

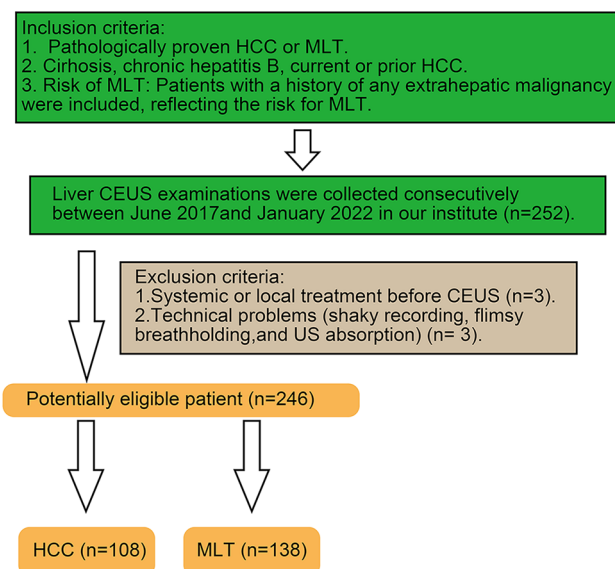


Figure 1. Flow chart of participant inclusion. CEUS: Contrast-enhanced ultrasound; HCC: Hepatocellular carcinoma; MLT: Metastatic liver tumor

Subgroup analysis

We divided liver lesions into two subgroups (≤ 3 cm and > 3 cm) based on their maximum diameters as measured by grayscale ultrasound at the peak of intensity phase of the CEUS, recognizing that the size of a lesion may influence its perfusion characteristics. According to histopathologic findings, the HCC group was divided into two subgroups (well and moderately differentiated and poorly and moderately-to-poorly differentiated) as HCCs with variable degrees of histologic differentiation may also exhibit different wash-in and wash-out characteristics. Due to the liver puncture biopsy, a small amount of the HCC differentiation data (12/138, 8.7%) was lost. Additionally, the MLT group was subdivided into two subgroups (hypervascular and hypovascular) based on the primary malignancy type. Neuroendocrine tumors, sarcomas, and malignant melanoma are the most common causes of hypervascular metastases, while colorectal, gastric, pancreatic, lung, and ovarian cancer are the most common causes of hypovascular metastases [11].

Ultrasound imaging acquisition

The CEUS examinations were conducted using a Philips iU22 ultrasound system (Philips Healthcare, Bothell, WA) with a C5-1 MHz transducer. The following parameters were used:

Mechanical Index (MI): Set between 0.05 and 0.08 to minimize microbubble destruction.

Position of Focus: Adjusted to the level of the lesion to optimize image clarity.

Frequency: The transducer operated at a frequency range of 1–5 MHz, with adjustments made based on the patient's body habitus and lesion depth.

A volume of 1.5 mL of contrast agent SonoVue (Bracco Suisse SA, Switzerland) was injected *via* an angiocatheter (20 G) implanted in the antecubital vein, followed by flushing with 5.0 mL of 0.9% saline. The target lesion was continuously scanned and imaged until liver parenchymal enhancement diminished, typically lasting at least 3 min. Continuous digital storage of real-time CEUS video frames was performed on a hard disk for further analysis.

Sonographer Expertise:

The CEUS examinations were performed by two experienced radiologists with extensive backgrounds in abdominal ultrasound and CEUS:

Radiologist 1 Weiqin Huang: 15 years of experience in abdominal ultrasound and CEUS.

Radiologist 2 Ruoxuan Lin: 11 years of experience in abdominal ultrasound and CEUS.

Both radiologists have undergone specialized training in CEUS techniques and have participated in numerous clinical studies and workshops on liver imaging.

The radiologists independently reviewed the CEUS features and liver imaging reporting and data system (LI-RADS) categories of the lesions. Disagreements were resolved through consensus.

Blinding to Clinical Data:

To ensure the objectivity of the imaging assessment, both radiologists were blinded to the patient's clinical data, including their medical history, laboratory results, and prior imaging findings, during the CEUS examination and image interpretation. This blinding procedure was implemented to prevent any potential bias and to ensure that the evaluation of the CEUS features and LI-RADS categories was solely based on the imaging findings.

CEUS image analysis

All CEUS images were reviewed independently by two experienced radiologists (15 and 6 years of experience, respectively). The clinical information and final histopathologic diagnosis were concealed from both radiologists.

During the arterial phase (AP), the wash-in patterns were classified as homogeneous or heterogeneous hyper-enhancement, peripheral rim-like hyper-enhancement, iso-enhancement, and hypo-enhancement when compared with the adjacent liver parenchyma. The arterial phase hyperenhancement (APHE) pattern refers to lesions with homogeneous or heterogeneous hyperenhancement in AP. In the CEUS LI-RADS v2017, peripheral rim-like hyper-enhancement refers to Rim APHE, which is a subtype of APHE. The term "washout" refers to a lesion becoming hypoechoic compared with the adjacent liver parenchyma. In order to obtain more detailed information, the onset time of wash-out after contrast injection was classified into three categories: < 45 s, 45 s to 1 min, and ≥ 1 min. The two categories of wash-out were mild and severe, with the latter referring to being virtually devoid of enhancement within 120 s.

Two radiologists further classified each lesion into relevant categories based on CEUS-LI-RADS v2017 [12].

The inter-reader agreement was evaluated after independent analysis. Disagreements between the two radiologists were resolved after discussion. To assess intra-reader variability, each radiologist independently re-evaluated a randomly selected subset of 30 liver lesions after an interval of four weeks, without access to their initial assessments. This approach was intended to minimize recall bias and to gauge the consistency of each reader's diagnostic interpretations over time. Inter-reader variability was evaluated by comparing the initial independent assessments of the liver lesions by the two radiologists. Any discrepancies between the readers were resolved through consensus after a joint review session, where both radiologists discussed each case until agreement was reached. The results of intra- and inter-reader variability assessments were quantified using the kappa (κ) statistic, which measures agreement beyond chance. A κ value of 0.81–1.00 was considered almost perfect agreement, 0.61–0.80 substantial agreement, 0.41–0.60 moderate agreement, 0.21–0.40 fair agreement, and ≤ 0.20 slight agreement.

To ensure the statistical rigor of our study, we conducted a power analysis to determine the appropriate sample size. Based on a preliminary data review and existing literature, our objective was to detect a clinically significant difference in the diagnostic efficacy of CEUS LI-RADS for distinguishing HCC from metastatic liver tumors. Aiming for a power of 80% and an alpha level of 0.05, our calculations suggested that a sample size of 95 was necessary. This size was deemed sufficient to observe the expected difference in diagnostic performance, considering the prevalence of HCC among individuals at risk and the diagnostic accuracy of CEUS LI-RADS reported in prior research. This power calculation underscores the robustness of our study design and supports the reliability of our findings.

Statistical analysis

The median and range are used to represent measurement data, while absolute numbers and percentages are used to represent categorical data. The Wilcoxon rank-sum test, Pearson's chi-squared test, or Fisher's exact test was used to compare differences between groups. The sensitivity, specificity, accuracy, positive predictive value (PPV), and negative predictive value (NPV) of LI-RADS categories were calculated. Two radiologists assessed inter-observer agreement by calculating the κ -value. IBM SPSS Statistics v.22 and MedCalc 20.010 were used for statistical analysis. A two-tailed P value of < 0.05 was considered statistically significant.

Results

Clinical characteristics and B mode Ultrasound (BUS) imaging features

A total of 246 patients with pathologically confirmed liver lesions, including 108 cases of HCCs and 138 cases of MLTs, were included in this study. All patients were pathologically diagnosed by surgical resection (40.24%) or needle biopsy (59.76%). Patients with HCC and MLT were distinguished by immunohistochemistry (IHC), shown in Figures S1 and S2.

Table 1 provides a summary of the clinical characteristics of the patients and the imaging features of the lesions. Liver cirrhosis was detected in 49.1% (53/108) of HCCs and 0.7% (1/138) MLTs ($P < 0.001$). Chronic hepatitis B was detected in 87.0% (94/108) of HCCs and 14.5% (20/138) MLTs ($P < 0.001$). HCCs are more prevalent in males ($P < 0.001$), and tumors in HCCs have a larger diameter ($p=0.003$). On conventional ultrasound, there were no statistically significant differences in the morphology, margin, or echo between the two groups.

LI-RADS categories and diagnostic performance

The sensitivity, specificity, and accuracy of LR-5 for the diagnosis of HCC were 49.1% (95% CI 39.3–58.9), 97.1% (95% CI 92.7–99.2), and 76%, respectively. The PPV of LR-5 for diagnosing HCC was 93.0% (95% CI 83.2–97.3).

Table 1. Study population baseline characteristics.

	HCC (n = 108)	MLT (n = 138)	<i>P</i>
Age (year), median(range)	55.72 (28–82)	56.72 (32–84)	0.934
Sex			
Male	97 (89.8%)	74 (53.6%)	<0.001*
Female	11 (10.2%)	64 (46.4%)	
Liver disease			
Cirrhosis	53 (49.1%)	1 (0.7%)	<0.001*
Chronic hepatitis B	94 (87.0%)	20(14.5%)	<0.001*
Size of hepatic tumors (cm), median (range)	6.28 (1.5–20.6)	4.27(0.8–15.2)	0.003*
Shape of hepatic tumors			
Round	64 (59.3%)	100 (72.5%)	0.029*
Lobulated or irregular	44 (40.7%)	38 (27.5%)	
Margin of hepatic tumors			
Clear	71 (65.7%)	98 (71.0%)	0.376
Ill-defined	37 (34.2%)	40 (29.0%)	
BUS echo			
Hypo-echo	79 (73.1%)	108 (78.3%)	0.665
Iso-echo	6 (5.5%)	7 (5.1%)	
Hyper-echo	20 (18.5%)	18 (13.0%)	
Mixed-echo	3 (2.8%)	5 (3.6%)	
Method of sampling			
Biospy	35 (32.4%)	51 (37.0%)	0.458
Sugery	73 (67.6%)	87 (63.0%)	
BMI, median (range)	22.1 (16.2–28.3)	21.5 (17.3–28.6)	0.384
Distance between skin and tumor (cm), median (range)	6.5 (1.2–14.5)	7.2 (1.1–13.8)	0.857

Data in parentheses are shown as percentages.

*Statistically significant.

Table 2. Frequencies of LI-RADS categories and diagnostic performances for HCC and MLT.

	LI-RADS categories				
	LR-3	LR-4	LR-5	LR-M	LR-TIV
HCC (n=108)	0 (0%)	18 (16.7%)	53 (49.1%)	30 (27.8%)	7 (6.5%)
MLT (n=138)	10 (7.2%)	1 (0.7%)	4 (2.9%)	123 (89.1%)	0 (0%)
Total	10 (4.1%)	19 (7.7%)	57 (23.2%)	153 (62.2%)	7 (2.8%)
PPV for diagnosis of HCC (95%CI)	0	94.7 (70.9–99.3)	93.0 (83.2–97.3)	19.6 (15.2–24.9)	100

	Diagnostic performances of LR-5 for HCC and LR-M for MLT				
	Accuracy	Sensitivity (95%CI)	Specificity (95% CI)	PPV (95% CI)	NPV (95% CI)
LR-5 for HCC	76.0	49.1 (39.3–58.9)	97.1 (92.7–99.2)	93.0 (83.2–97.3)	70.9 (66.9–74.6)
LR-M for MLT	81.7	89.1 (82.7–93.8)	72.2 (62.8–80.4)	80.4 (75.1–84.8)	83.9 (76.1–89.5)

LI-RADS Liver Imaging Reporting and Data System, HCC hepatocellular carcinoma, MLT metastatic liver tumors, CI confidence interval, PPV positive predictive value, NPV negative predictive value.

Table 3. The wash-in and washout features of HCC and MLT groups.

		HCC (n=108)	MLT (n=138)	P
Wash-in patterns	APHE	107 (99.1%)	95 (68.8%)	<0.001*
	Rim APHE	0 (0%)	21 (15.2%)	
	Iso-	1 (0.9%)	11 (8.0%)	
	Hypo-	0 (0%)	11 (8.0%)	
	Total	108	138	
Degree of washout	Mild	84 (77.8%)	20 (14.5%)	<0.001*
	Marked	6 (5.6%)	107 (77.5%)	
	No washout	18 (16.7%)	11 (8.0%)	
	Total	108	138	
Washout onset	<45s	13 (14.4%)	78 (61.4%)	<0.001*
	45-1min	18 (20.0%)	45 (35.4%)	
	≥1min	59 (65.6%)	4 (3.2%)	
	Total	90	127	

Data in parentheses are shown as percentages.

*Statistically significant.

Table 2 displays the sensitivity, specificity, and accuracy of LR-M for the diagnosis of MLT: 89.1% (95% CI 82.7–93.8), 72.2% (95% CI 62.8–80.4), and 81.7%, respectively. Only a small proportion of MLTs was assigned as LR-3 (10/138, 7.2%), LR-4 (1/138, 0.7%), and LR-5 (4/138, 2.9%), demonstrating high positive predictive values of 80.4 (95%CI 75.1–84.8%) for diagnosing MLT. Ten LR-3 observations were all MLT, whereas seven LR-TIV lesions were HCCs.

CEUS features

The CEUS characteristics of HCC and MLT are presented in Table 3. Arterial phase APHE was predominant in 99.1% of HCCs compared to 68.8% of MLTs ($p < 0.001$) (Figures 2 and 3), whereas 15.2% of MLTs and none of the HCCs exhibited Rim APHE. Iso-echo was observed in 11 (8.0%) of the MLT lesions

compared with only 1 HCC lesion, while hypo-echo was similarly observed in MLT (8.0%) but not seen in HCC ($p < 0.001$).

In terms of washout onset, 96.8% of MLTs exhibited early washout with an onset time of less than 60s, and 61.6% of MLTs exhibited washout onset time before 45s. In contrast, washout onset later than 60s was observed in 65.6% of HCCs ($p < 0.001$) (Table 3) (Figures 1 and 2). Only 4 (3.2%) cases of MLT exhibited washout after 60s, and 3 of them were hypervascular metastases.

In terms of the degree of washout, more MLTs (77.5%) than HCCs displayed marked washout, while more MLTs (77.8%) showed mild washout ($p < 0.001$) (Table 3).

Subgroup analysis

In the HCC subgroup, there were no statistically significant differences in the LR category based on nodule size and level of differentiation ($p = 0.539$ and 0.134 , respectively) (Table 4). However, the distribution of LR classification in the MLT subgroup was affected by tumor size ($p = 0.037$). In our cohort, there were more LR-3 lesions ≤ 3 cm (7/57, 12.8%) while only 0.37% in lesions > 3 cm. Interestingly, 10 cases of metastatic tumors were categorized as LR-3, with 9 of them having hypovascular primary tumors (Figure 4).

In the HCC subgroup, there were no statistically significant differences in the enhancement pattern based on nodule size and degree of differentiation (Table 5). However, all poorly and moderate-to-poorly differentiated HCC lesions displayed washout signs at some stage, whereas well and moderately differentiated HCC exhibited no washout. Half of the poorly and moderate-to-poorly differentiated HCC demonstrated early washout (< 60 s) and were classified as LR-M. In the MLT subgroup, 10 of 11 MLTs showing no washout were associated with hypovascular primary malignancies, whereas 3 of 4 MLTs showing washout after the 60s were nodules commonly considered to be of the hypervascular type.

Discussion

In this study, we aimed to assess the diagnostic performance of CEUS-LI-RADS v2017 in differentiating HCC from metastases in high-risk patients with chronic liver disease and extrahepatic malignancy. Adding a study population with a current or prior history of extrahepatic malignancy to the defined LI-RADS applicable population did not affect the high specificity (97.1%)

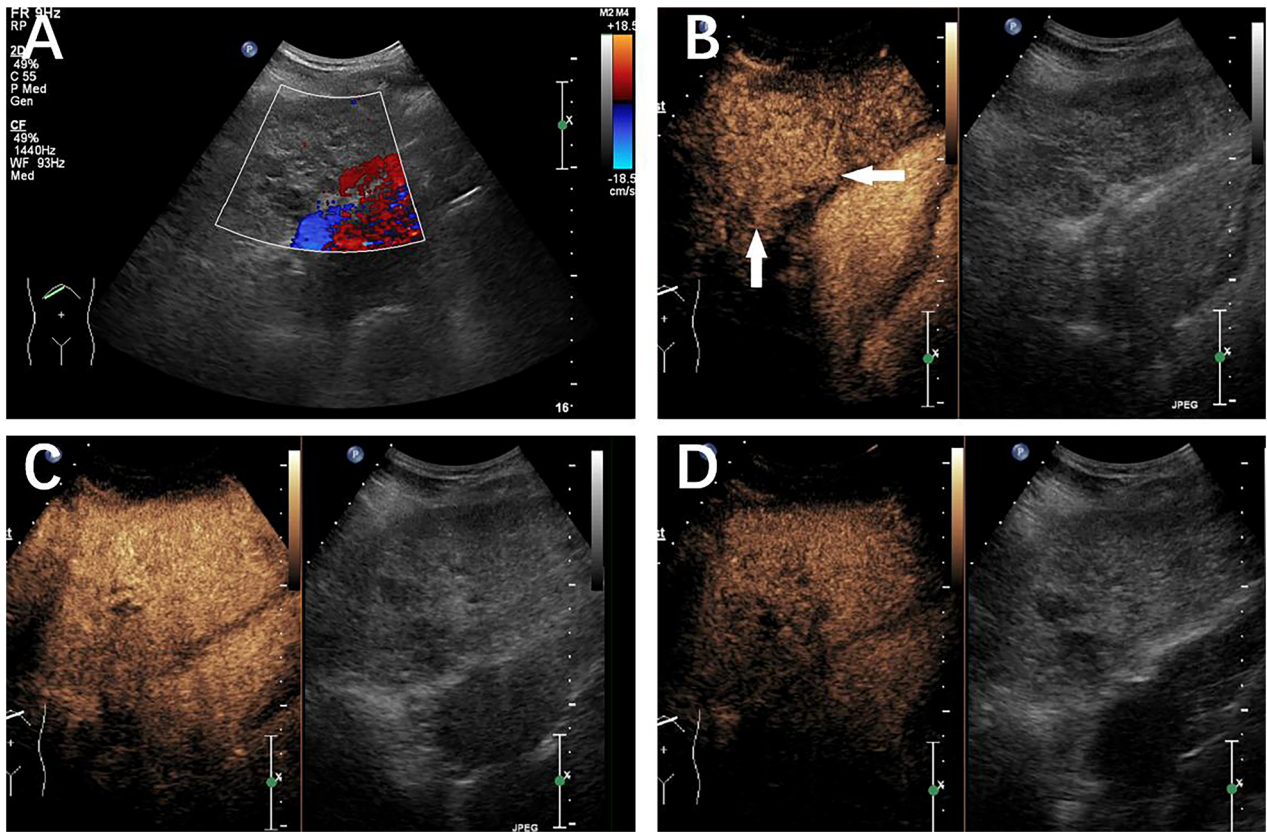


Figure 2. A liver lesion categorized as LR-5 was identified in a 61-year-old male with chronic hepatitis B. Well-differentiated hepatocellular carcinoma (HCC) was verified by histopathology. (A) B-mode ultrasound detected a mixed hypoechoic nodule 4.9cm in diameter in the left lobe of the liver. (B) 23s after SonoVue injection, homogeneous APHE (white arrow) was observed. (C) In the early portal phase at 60s, iso-enhancement compared to the adjacent liver parenchyma was observed. (D) Mild washout was present at 180s after SonoVue injection.

of LR-5 for the diagnosis of HCC. In addition, the LR-M category demonstrated a high level of sensitivity (89.1%) and diagnostic accuracy (81.7%) for metastasis. It is feasible to expand the use of CEUS-LI-RADS in distinguishing HCC from MLT in such individuals, as evidenced by our results that CEUS-LI-RADS is a valuable tool. In our results, the diagnostic performance metrics (sensitivity, specificity, and accuracy) reflect the combined use of B-mode and CEUS. The high specificity observed in our study indicates that B-mode imaging, when used in conjunction with CEUS, does not compromise but rather supports the accurate differentiation of HCC from liver metastasis. For instance, B-mode imaging's ability to provide clear anatomical context helps in differentiating benign features from malignant vascular patterns observed in CEUS, thereby enhancing overall diagnostic confidence. The use of B-mode imaging alongside CEUS in our study likely contributed positively to the diagnostic performance. The morphological details obtained from B-mode imaging complement the vascular characteristics observed in CEUS, leading to a more accurate and reliable assessment of liver lesions. Therefore, we believe that B-mode

imaging, when integrated with CEUS, enhances the diagnostic process and should be considered an integral part of liver lesion evaluation.

With a sensitivity of 74% and a specificity of 89%, LR-5 was able to distinguish HCC from non-HCC cancers in cirrhotic livers, according to research involving fewer than 10 metastatic patients [6]. Our findings are comparable to those of other research that evaluated the diagnostic performance of distinguishing HCC from non-HCC hepatic cancers [6,13,14], although the sensitivity in our study is relatively low (49.1%). We believe it is because a small proportion of HCC was classified as LR-M due to the presence of early washout (45–60s) based on the current LR-M criteria. HCCs were detected in 93.0% of the LR-5 observations in our study. This finding is consistent with the meta-analysis [15], which determined that in a target sample of patients who were predominantly free of extrahepatic malignancy, 94.0% of LR-5 observations were HCCs. Notably, the inclusion of patients at risk for metastases did not reduce the PPV of the LR-5 diagnosis in our study, however, LI-RADS should be applied with caution for such patients [16].

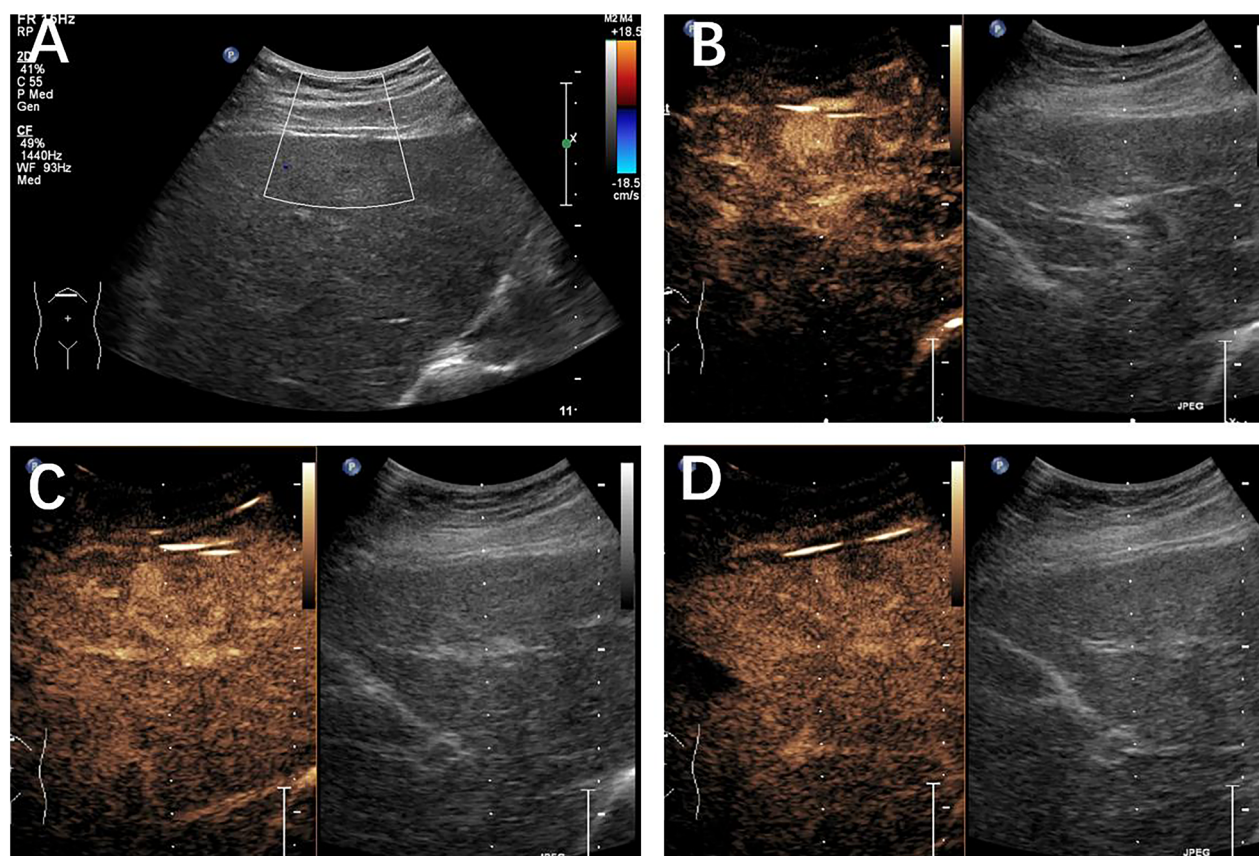


Figure 3. A 49-year-old female patient with a history of nasopharyngeal cancer with a liver lesion categorized as LR-M. Histopathology confirmed the presence of a metastasized liver tumor. (A) B-mode ultrasound detected a hypoechoic mass 2.1 cm in diameter located in the left lobe of the liver. (B) Homogeneous APHE was observed 21 s after SonoVue injection. (C) Early washout (white arrow) was observed at 43 s after SonoVue injection. (D) A marked washout was observed at 90 s after SonoVue injection.

Table 4. Subgroup analysis of LR-category based on nodule size, degree of differentiation and blood supply.

	LR-3	LR-4	LR-5	LR-M	LR-TIV	Total	<i>P</i>	
HCC	≤3cm	–	5	10	4	21	0.539	
			(23.8%)	(47.6%)	(19.0%)	(9.5%)		(100%)
	>3cm	–	15	43	26	5	87	0.134
			(17.2%)	(49.4%)	(29.9%)	(5.7%)	(100%)	
WD and MD	–	14	45	22	3	84	0.134	
		(16.7%)	(53.6%)	(26.2%)	(3.6%)	(100%)		
PD and MPD	–	0	5	6	1	12	0.037*	
		(0.0%)	(41.7%)	(50.0%)	(0.8%)	(100%)		
MLT	≤3cm	7	1	0	49	–	57	0.037*
		(12.3%)	(1.8%)	(0.0%)	(86.0%)		(100%)	
	>3cm	3	0	4	74	–	81	0.091
		(3.7%)	(0.0%)	(4.9%)	(91.4%)		(100%)	
Hypo-vascular	9	1	1	86	–	97	0.091	
	(9.3%)	(1.0%)	(1.0%)	(88.7%)		(100%)		
Hyper-vascular	1	0	3	37	–	41	0.091	
	(2.4%)	(0.0%)	(7.3%)	(90.2%)		(100%)		

Data in parentheses are shown as percentages.

WD: well differentiated, MD: moderately differentiated, PD: poorly differentiated, MPD: moderately-to-poorly differentiated.

*Statistically significant.

Early discharge has been associated with poorly-differentiated HCCs or non-hepatocellular malignancies [17–19], which is consistent with our observation. Among those poorly and moderate-to-poorly differentiated HCCs, half of the lesions (6/12, 50%)

were classified as LR-M, indicating that poorly differentiated HCC may be more susceptible to early washout (45 s–60 s) [10]. As suggested in a previous study [20], modifying the current LR-M criteria can enhance specificity. However, this method may misclassify some

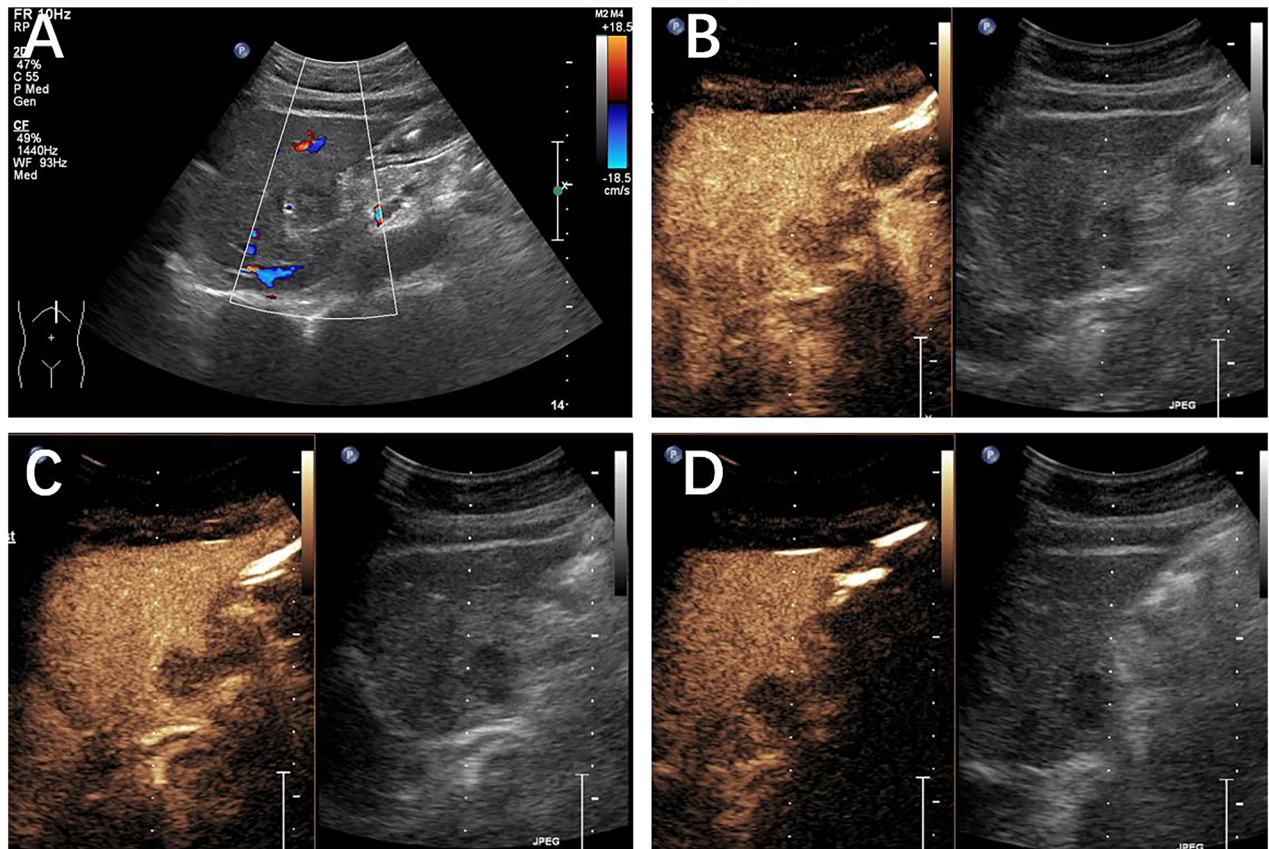


Figure 4. Histopathology confirmed the presence of a metastatic liver tumor in a 56-year-old female patient with a history of lung cancer. (A) A hypoechoic mass was discovered within the left lobe. On CEUS, the mass exhibited hypo-enhancement during the arterial phase (B), the portal venous phase (60s) (C), and the late phase (2min) (D). The lesion was classified as LR-3 based on the CEUS LI-RADS guidelines.

Table 5. Subgroup analysis of CEUS imaging features based on nodule size, degree of differentiation and blood supply.

		Wash-in pattern			<i>P</i>	Washout onset				<i>P</i>	
		APHE	Rim APHE	Iso/ Hypo		No	<45s	45s-1 Min	≥1min		
HCC	≤3cm	20 (95.2%)	0 (0.0%)	1 (4.8%)	0.194	5 (23.8%)	2 (9.5%)	2 (9.5%)	12 (57.1%)	0.656	
	>3cm	87 (100%)	0 (0.0%)	0 (0.0%)		13 (14.9%)	11 (12.6%)	16 (18.4%)	47 (54.0%)		
	WD and MD	84 (100%)	0 (0.0%)	0 (0.0%)	14 (16.7%)	9 (10.7%)	14 (16.7%)	47 (56.0%)	0.212		
	PD and MPD	12 (100%)	0 (0.0%)	0 (0.0%)	0 (0.0%)	3 (25.0%)	3 (25.0%)	6 (50.0%)			
MLT	≤3cm	37 (64.9%)	8 (14.0%)	12 (21.1%)	0.387	7 (12.3%)	33 (57.9%)	17 (29.8%)	0 (0.0%)	0.168	
	>3cm	58 (71.6%)	13 (16.0%)	10 (12.3%)		4 (4.9%)	45 (55.6%)	28 (34.6%)	4 (4.9%)		
	Hypo-vascular	66 (68.0%)	17 (17.5%)	14 (14.4%)	0.440	10 (10.3%)	55 (56.7%)	31 (32.0%)	1 (0.1%)		0.107
	Hyper-vascular	29 (70.7%)	4 (9.8%)	8 (19.5%)		1 (2.4%)	23 (56.1%)	14 (34.1%)	3 (7.3%)		

Data in parentheses are shown as percentages.

WD: well differentiated, MD: moderately differentiated, PD: Poorly differentiated, MPD: moderately-to-poorly differentiated.

*Statistically significant.

MLTs as LR-5 in patients at risk for both HCC and MLT, and it must be validated in future research. The LR-M category demonstrated high diagnostic accuracy (81.7%) for metastases. Rim APHE was once regarded as the hallmark of MLT, particularly for hypovascular

metastases. However, these findings were usually based on CT or MRI. In our study, the most frequently observed enhancement patterns were APHE followed by early washout, which was consistent with prior research [21]. CEUS images clearly demonstrate the

continuous dynamic enhancement pattern, whereas CT and MRI may overlook the actual hypervascularization of arterial vessels. Significant and early washouts were more prevalent in MLTs than in HCCs. According to our investigation, 78 (61.4%) metastasis lesions experienced washout within the first 45s and 45 (35.4%) between 45 and 60s. This indicated that the hyper-enhancement of MLTs was only a transient phenomenon. The comparatively low volume of the lesions, the efficient venous drainage, the characterization of the microvasculature [22], and the absence of portal vein supply [23], may all contribute to the rapid elimination of MLTs.

According to previous research, the CEUS appearance of MLTs may be dependent on the type of primary malignancy [24] and the size of the lesion [21]. In our study, the proportions of LR-categories in the MLT group were demonstrated to be correlated with lesion magnitude. In addition, the pattern of enhancement may also reflect the tumor vascularity of metastases. LR-3 metastases are characterized by their diminutive size and hypovascular supply. Three of the four LR-5 metastatic nodules that exhibited washout after 60s originated from neuroendocrine tumors, sarcomas, and malignant melanoma, which are all commonly believed to be hypervascular nodules. Some small and hypovascular metastases may exhibit iso- and hypo-enhancement during the arterial phase and be classified as LR-3 and LR-4 as they have fewer feeding vessels. Long-lasting arterial enhancement in hypervascular metastases is a result of the enhanced arterial flow partially compensating for the decreased portal venous flow in liver lesions [25]. Recent research by Cao et al. [26] found that Sonazoid®-modified LR-5 had better diagnostic sensitivity for HCC compared to SonoVue® LR-5, suggesting that alternative contrast agents may enhance the diagnostic performance of CEUS-LI-RADS.

On the other hand, incorporating the LI-RADS tumor in vein (TIV) criteria into our analysis has significantly enhanced our understanding of the diagnostic landscape for hepatocellular carcinoma within the context of CEUS. The identification of TIV, a hallmark of advanced HCC, underscores the aggressive nature of the disease and the necessity for prompt, potentially curative treatments. Our findings suggest that CEUS LI-RADS, with its capability to detect TIV, offers a robust framework for the assessment of HCC severity, thereby facilitating tailored patient management and intervention strategies. This addition to our study underscores the importance of comprehensive diagnostic criteria, such as LI-RADS, in the nuanced differentiation between HCC and metastatic liver tumors,

providing a foundation for improved patient outcomes through informed clinical decision-making. The CEUS LI-RADS criteria incorporate a range of ancillary features that can be utilized to increase or decrease confidence in HCC diagnosis. These features include but are not limited to the presence of intralesional fat, blood flow in the perilesional area, and the visibility of a 'tumor in vein' sign. Ancillary features can significantly aid in characterizing liver lesions, especially in cases where the primary LI-RADS features (such as arterial phase hyperenhancement and portal venous phase washout) provide equivocal results. Our study acknowledges the critical role of these ancillary features in enhancing diagnostic accuracy and confidence, particularly in distinguishing HCC from MLT. By integrating ancillary features into our analysis, we aim to highlight their significance in the CEUS LI-RADS framework and advocate for their systematic assessment as part of a comprehensive diagnostic strategy for liver lesions.

We acknowledge the relatively low incidence of metastasis in cirrhotic livers observed in our cohort. This phenomenon may be partly explained by Stephen Paget's 'seed and soil' hypothesis, which suggests that the metastatic potential of cancer cells ('seeds') is significantly influenced by the compatibility with the microenvironment of the host tissue ('soil'). In the context of liver cirrhosis, the altered hepatic architecture and microenvironment might not be conducive for the implantation and growth of metastatic cells from extrahepatic primary tumors. Furthermore, cirrhosis often leads to a shift in vascular dominance from the portal vein to the hepatic artery, altering the liver's blood supply. This vascular remodeling could further limit the hepatic entry of metastatic cells *via* the portal vein, traditionally considered the primary route for liver metastases. Incorporating these considerations, our findings suggest a complex interplay between the cirrhotic liver's altered vascular and tissue environments and the relatively uncommon occurrence of metastasis in such patients.

There are some limitations to our study. First, the retrospective, single-center design introduced a degree of selection bias. Future prospective and multicenter studies are required to further validate the current recommendations. Second, although only pathology-proven HCCs and metastases were included in our study, it is possible that our diagnostic findings do not precisely reflect what would be observed in real-world situations. However, the purpose of this study was to evaluate and validate the applicability of CEUS-LI-RADS in patients at risk for both HCC and metastases. In addition, although the inclusion of

benign hepatic nodules in our study was an ideal choice, there were significant logistical and methodological challenges. Within the scope of our current study, retrospective collection of a sufficiently large and representative sample of benign lesions with complete CEUS data and pathological confirmation was not feasible. We acknowledge this limitation and suggest that future prospective studies could be designed to include benign hepatic nodules, thereby further improving the utility of CEUS-LI-RADS in a broader clinical context. Lastly, the proportion of LR-3-type and LR-4-type nodules in this study was quite low due to pathological reasons, and selection bias may have been introduced.

Conclusion

Our investigation showed that CEUS-LI-RADS is a useful tool with a high specificity for distinguishing HCC from MLT in an expanding population, namely patients with chronic liver disease and extrahepatic malignancy. Based on current LR-M criteria, a small proportion of HCC cases may be classified as LR-M due to the presence of early washout (45–60s). Metastases categorized as LR-3 are characterized by their diminutive size and hypovascular supply.

Acknowledgments

We would like to acknowledge the hard and dedicated work of all the staff who implemented the intervention and evaluation components of the study.

Disclosure statement

The authors declare that they have no competing interests.

Ethics approval and consent to participate

This study was approved by the Ethics Committee of the Clinical Oncology School of Fujian Medical University (No. K2022-168-01). This study was conducted in accordance with the Declaration of Helsinki. Written informed consent was obtained from all the participants.

Consent for publication

Not applicable.

Availability of data and materials

The datasets used and/or analyzed during the current study are available from the corresponding author upon reasonable request. We declare that the materials described in the

manuscript, including all relevant raw data, will be freely available to any scientist wishing to use them for non-commercial purposes without breaching participant confidentiality.

Authors contributions

Conception and design of the research: Weiqin Huang, Ruoxuan Lin

Acquisition of data: Weiqin Huang, Ruoxuan Lin, Zhongshi Du, Zhougui Wu, Xiaohui Ke

Analysis and interpretation of the data: Weiqin Huang, Zhongshi Du, Lina Tang, Zhougui Wu, Xiaohui Ke

Statistical analysis: Weiqin Huang

Obtaining financing: Weiqin Huang, Ruoxuan Lin

Writing of the manuscript: Weiqin Huang

Critical revision of the manuscript for intellectual content: Weiqin Huang, Lina Tang

All authors read and approved the final draft.

Funding

This work was supported by the Joint Funds for Innovation of Science and Technology of Fujian Province. (grant number: 2021Y9220), the Fujian Provincial Health Commission (grant number: 2018-ZQN-14) and Startup Fund for scientific research, Fujian Medical University (Grant number: 2022QH1162).

References

- [1] Li X, Ramadori P, Pfister D, et al. The immunological and metabolic landscape in primary and metastatic liver cancer. *Nat Rev Cancer*. 2021;21(9):541–557. doi: [10.1038/s41568-021-00383-9](https://doi.org/10.1038/s41568-021-00383-9).
- [2] Schipilliti FM, Garajová I, Rovesti G, et al. The growing skyline of advanced hepatocellular carcinoma treatment: a review. *Pharmaceuticals (Basel)*. 2021;14(1):43. doi: [10.3390/ph14010043](https://doi.org/10.3390/ph14010043).
- [3] Kudo M, Trevisani F, Abou-Alfa GK, et al. Hepatocellular carcinoma: therapeutic guidelines and medical treatment. *Liver Cancer*. 2016;6(1):16–26. doi: [10.1159/000449343](https://doi.org/10.1159/000449343).
- [4] Kono Y, Lyschchik A, Cosgrove D, et al. Contrast Enhanced Ultrasound (CEUS) Liver Imaging Reporting and Data System (LI-RADS®): the official version by the American College of Radiology (ACR). *Ultraschall Med*. 2017;38(1):85–86. doi: [10.1055/s-0042-124369](https://doi.org/10.1055/s-0042-124369).
- [5] Chernyak V, Fowler KJ, Kamaya A, et al. Liver Imaging Reporting and Data System (LI-RADS) version 2018: imaging of hepatocellular carcinoma in at-risk patients. *Radiology*. 2018;289(3):816–830. doi: [10.1148/radiol.2018181494](https://doi.org/10.1148/radiol.2018181494).
- [6] Kim Y-Y, Kim M-J, Kim EH, et al. Hepatocellular carcinoma versus other hepatic malignancy in cirrhosis: performance of LI-RADS version 2018. *Radiology*. 2019;291(1):72–80. doi: [10.1148/radiol.2019181995](https://doi.org/10.1148/radiol.2019181995).
- [7] Dopazo C, Søreide K, Rangelova E, et al. Hepatocellular carcinoma. *Eur J Surg Oncol*. 2024;50(1):107313. doi: [10.1016/j.ejso.2023.107313](https://doi.org/10.1016/j.ejso.2023.107313).

- [8] Tanaka H. Current role of ultrasound in the diagnosis of hepatocellular carcinoma. *J Med Ultrason* (2001). 2020;47(2):239–255. Epub 2020 Mar 13. PMID: 32170489; PMCID: PMC7181430. doi: [10.1007/s10396-020-01012-y](https://doi.org/10.1007/s10396-020-01012-y).
- [9] Motz VL, White R, Lee R, et al. Contrast-enhanced ultrasound for screening hepatocellular carcinoma: an implemented program at a semi-rural academic center. *Abdom Radiol (NY)*. 2021;46(9):4170–4177. PMCID: PMC8100745. doi: [10.1007/s00261-021-03104-w](https://doi.org/10.1007/s00261-021-03104-w).
- [10] Pan JM, Chen W, Zheng YL, et al. Tumor size-based validation of contrast-enhanced ultrasound liver imaging reporting and data system (CEUS LI-RADS) 2017 for hepatocellular carcinoma characterizing. *Br J Radiol*. 2021;94(1126):20201359. doi: [10.1259/bjr.20201359](https://doi.org/10.1259/bjr.20201359).
- [11] Dănilă M, Popescu A, Sirli R, et al. Contrast enhanced ultrasound (CEUS) in the evaluation of liver metastases. *Med Ultrason*. 2010;12(3):233–237.
- [12] American College of Radiology. American College of Radiology CEUS LI-RADS®v2017 CORE. [accessed 2021 April 15].
- [13] Fraum TJ, Tsai R, Rohe E, et al. Differentiation of hepatocellular carcinoma from other hepatic malignancies in patients at risk: diagnostic performance of the liver imaging reporting and data system version 2014. *Radiology*. 2018;286(1):158–172. doi: [10.1148/radiol.2017170114](https://doi.org/10.1148/radiol.2017170114).
- [14] Zhou Y, Qin Z, Ding J, et al. Risk stratification and distribution of hepatocellular carcinomas in CEUS and CT/MRI LI-RADS: a meta-analysis. *Front Oncol*. 2022;12:873913. doi: [10.3389/fonc.2022.873913](https://doi.org/10.3389/fonc.2022.873913).
- [15] Van Der Pol CB, Lim CS, Sirlin CB, et al. Accuracy of the liver imaging reporting and data system in computed tomography and magnetic resonance image analysis of hepatocellular carcinoma or overall malignancy—a systematic review. *Gastroenterology*. 2019;156(4):976–986. doi: [10.1053/j.gastro.2018.11.020](https://doi.org/10.1053/j.gastro.2018.11.020).
- [16] Kim MJ, Lee S, An C. Problematic lesions in cirrhotic liver mimicking hepatocellular carcinoma. *Eur Radiol*. 2019;29(9):5101–5110. doi: [10.1007/s00330-019-06030-0](https://doi.org/10.1007/s00330-019-06030-0).
- [17] Fan ZH, Chen MH, Dai Y, et al. Evaluation of primary malignancies of the liver using contrast-enhanced sonography: correlation with pathology. *AJR Am J Roentgenol*. 2006;186(6):1512–1519. doi: [10.2214/ajr.05.0943](https://doi.org/10.2214/ajr.05.0943).
- [18] Yang D, Li R, Zhang XH, et al. Perfusion characteristics of hepatocellular carcinoma at contrast-enhanced ultrasound: influence of the cellular differentiation, the tumor size and the underlying hepatic condition. *Sci Rep*. 2018;8(1):4713. doi: [10.1038/s41598-018-23007-z](https://doi.org/10.1038/s41598-018-23007-z).
- [19] Huang J-Y, Li J-W, Lu Q, et al. Diagnostic accuracy of CEUS LI-RADS for the characterization of liver nodules 20 mm or smaller in patients at risk for hepatocellular carcinoma. *Radiology*. 2020;294(2):329–339. doi: [10.1148/radiol.2019191086](https://doi.org/10.1148/radiol.2019191086).
- [20] Li F, Li Q, Liu Y, et al. Distinguishing intrahepatic cholangiocarcinoma from hepatocellular carcinoma in patients with and without risks: the evaluation of the LR-M criteria of contrast-enhanced ultrasound liver imaging reporting and data system version 2017. *Eur Radiol*. 2020;30(1):461–470. doi: [10.1007/s00330-019-06317-2](https://doi.org/10.1007/s00330-019-06317-2).
- [21] Kong WT, Ji ZB, Wang WP, et al. Evaluation of liver metastases using contrast-enhanced ultrasound: enhancement patterns and influencing factors. *Gut Liver*. 2016;10(2):283–287. doi: [10.5009/gnl14324](https://doi.org/10.5009/gnl14324).
- [22] Murphy-Lavallee J, Jang HJ, Kim TK, et al. Are metastases really hypovascular in the arterial phase? The perspective based on contrast-enhanced ultrasonography. *J Ultrasound Med*. 2007;26(11):1545–1556. doi: [10.7863/jum.2007.26.11.1545](https://doi.org/10.7863/jum.2007.26.11.1545).
- [23] Larsen LP. Role of contrast enhanced ultrasonography in the assessment of hepatic metastases: a review. *World J Hepatol*. 2010;2(1):8–15. doi: [10.4254/wjh.v2.i1.8](https://doi.org/10.4254/wjh.v2.i1.8).
- [24] Claudon M, Cosgrove D, Albrecht T, et al. Guidelines and good clinical practice recommendations for contrast enhanced ultrasound (CEUS) - update 2008. *Ultraschall Med*. 2008;29(1):28–44. doi: [10.1055/s-2007-963785](https://doi.org/10.1055/s-2007-963785).
- [25] Mörk H, Ignee A, Schuessler G, et al. Analysis of neuroendocrine tumour metastases in the liver using contrast enhanced ultrasonography. *Scand J Gastroenterol*. 2007;42(5):652–662. doi: [10.1080/00365520601021765](https://doi.org/10.1080/00365520601021765).
- [26] Cao J, Wang H, Ling W. Compared with SonoVue® LR-5, Sonazoid® modified LR-5 has better diagnostic sensitivity for hepatocellular carcinoma: a systematic review and meta-analysis. *Quant Imaging Med Surg*. 2024;14(4):2978–2992. doi: [10.21037/qims-23-1616](https://doi.org/10.21037/qims-23-1616).